11th World Congress on Computational Mechanics (WCCM XI)
5th European Conference on Computational Mechanics (ECCM V)
6th European Conference on Computational Fluid Dynamics (ECFD VI)
E. Oñate, J. Oliver and A. Huerta (Eds)

MACROSCOPIC AND MESOSCOPIC MODELING BASED ON THE CONCEPT OF GENERALIZED STRESSES FOR CUTTING SIMULATIONS

R. Mahnken*, C. Cheng*, M. Düsing*, I. M. Ivanov† and E. Uhlmann†

* Chair of Engineering Mechanics (LTM),
University of Paderborn,
Warburgerstr. 100, 33098 Paderborn, Germany,
e-mail: mahnken@ltm.upb.de, web page: http://www.ltm.uni-paderborn.de/

†Institute for Machine Tools and Factory Management (IWF),
Technical University Berlin,
Pascalstraße, 10587 Berlin, Germany
e-mail: ivanmitkov.ivanov@iwf.tu-berlin.de - Web page: http://www.iwf.tu-berlin.de/

Key words: generalized stresses, gradient term, additional degree of freedom, asymmetric effects, transformation-induced plasticity, cutting simulation

Abstract. Based on the concept of generalized stresses proposed by Gurtin [5] and Forest *et al.* [4] macro- and meso-scopic modeling approaches are considered. A generalized principle of virtual power is postulated involving generalized stresses which are used to derive the constitutive equations for both approaches. For macroscopic modeling we develop a multi-mechanism model for a strain rate- and temperature dependent plastic material behavior accompanied by a Strength-Difference-effect (SD-effect) and the trip-strain due to phase transformation. Furthermore, we extend this model with the gradient of a phase fraction, which renders an extra degree of freedom in the finite element formulation. For mesoscopic modeling a phase field model is implemented for describing phase transformations. For the scenario of a cutting process we have a martensite-austenite-martensite transformation. In the examples we present finite element results for a cutting simulation and for a related phase field simulation.

1 Introduction

High speed cutting is being widely used in metal working, in which the work piece is machined under high speed causing highly inhomogeneous strain rates and temperature. Due to phase transformations under the intense, localized, rapid thermal-mechanical loading, white and dark layers are induced, which determine the mechanical properties of the workpiece. To describe the material behavior, many macroscopic models were developed over last years. A simple model by Dudzinski and Molinari [3] considers the shearing produced during the chip formation in orthogonal cutting. Sievert *et al.* [13] consider ductile damage at high strain-rates and the influence of the stress-triaxiality on ductile damage. Marusich and Ortiz [11] introduce a Lagrangian finite element model with remeshing. In addition, more physically-based models are available, such as the Zerilli-Armstrong model [15], which is based on simplified dislocation mechanics. Ramesh and Melkote [12] predict the thickness of white layer taking into account the effects of stress and strain on phase transformation temperatures, where martensitic phase transformation accompanied by the transformation-induced plasticity (TRIP) effect was considered.

Gurtin [5] formulate phase field models within a continuum thermodynamic framework, where microforces associated with the order parameter and its first gradient are introduced. Based on additional degrees of freedom and generalized stresses, Forest *et al.* [4] describe a thermodynamic consistent phase field model, which is extended with gradient terms. It is demonstrated, that there are strong links between generalized continuum mechanics and phase field models which are striving in modern field theories of materials. As a special case, the order parameter which describes phase changes in a mesoscopic modelling can be regarded as a phase fraction for macroscopic modelling.

Based on this theory, the multi-mechanism model of our previous work [10] can be extended by an additional degree of freedom, the phase fraction. Furthermore, the influence of its first gradient on the visco-plastic material behavior is an essential aim of this work. This paper is organized as follows:

- Section 2 presents a constitutive framework for macroscopic and mesoscopic modelling based on the concept of generalized stresses according to [4]. Using the principle of virtual power the balance relations of the generalized stresses are derived. Additionally the Clausius-Duhem inequality is formulated. The evolution equations are generally formulated in accordance with the Clausius-Planck inequality in order to obtain a thermodynamic consistent model.

- In the examples in Section 3 a cutting simulation at the macrolevel and a phase-field simulation at the mesolevel are presented.

Notations

Square brackets $[\bullet]$ are used throughout the paper to denote 'function of' in order to distinguish from mathematical groupings with parenthesis $(\bullet)$.

2 Macroscopic and mesoscopic modelling based on the concept of generalized stresses

2.1 General setting

According to GURTIN's theory [5], there exists a scalar internal microstress π and a vector microstress $\boldsymbol{\xi}$. For a mesoscopic formulation, they perform work in conjunction with changes in the configurations of atoms, characterized by a chemical variable, the order parameter ϕ, and its first gradient $\nabla\phi$. For a macroscopic case, the phase volume fraction z_A is regarded as the chemical variable representing the austenite volume fraction. Considering a non-isothermal formulation the degrees of freedom for both cases are

$$1.\ \mathrm{DOF}_{macro} = \{\mathbf{u},\ \ \theta,\ \ z_A\} \quad 2.\ \mathrm{DOF}_{meso} = \{\mathbf{u},\ \ \theta,\ \ \phi\}, \tag{1}$$

where $\mathbf{u}$ is the displacement and θ the temperature. A first gradient theory is built on

$$\begin{array}{lll} 1. & \mathrm{STRAIN}_{macro} & = \{\boldsymbol{\varepsilon},\ \ \theta,\ \ \nabla\theta,\ \ z_A,\ \ \nabla z_A\} \\ 2. & \mathrm{STRAIN}_{meso} & = \{\boldsymbol{\varepsilon},\ \ \theta,\ \ \nabla\theta,\ \ \phi,\ \ \nabla\phi\}, \end{array} \tag{2}$$

where $\boldsymbol{\varepsilon}$, the total strain tensor, is the symmetric part of the displacement gradient.

According to AMMAR *et al.* [1] the principle of virtual power for the macroscopic case is as follows:

$$\begin{array}{lll} 1. & \mathcal{P}^{(i)}[\delta z_A, \delta\mathbf{u}, V] & = \int_V p^{(i)}[\delta z_A, \delta\mathbf{u}]dv \\ 2. & \mathcal{P}^{(e)}[\delta z_A, \delta\mathbf{u}, V] & = \int_V p^{(e)}[\delta z_A, \delta\mathbf{u}]dv \\ 3. & \mathcal{P}^{(c)}[\delta z_A, \delta\mathbf{u}, V] & = \int_{\partial V} p^{(c)}[\delta z_A, \delta\mathbf{u}]ds \end{array} \tag{3}$$

for all subdomains $\mathcal{D}$ of the body V. Here $\mathcal{P}^{(i)}$, $\mathcal{P}^{(e)}$ and $\mathcal{P}^{(c)}$ are the overall virtual powers of internal, external and contact generalized forces, and $p^{(i)}$, $p^{(e)}$ and $p^{(c)}$ are related densities, respectively. δz_A and $\delta\mathbf{u}$ represent the virtual volume phase fraction and the virtual displacement. With generalized stresses $\{-\pi, \boldsymbol{\xi}, \boldsymbol{\sigma}\}$ and its power-conjugates $\{\delta z_A, \nabla\delta z_A,\ \nabla\delta\mathbf{u}\}$ *the virtual power densities of internal* and *external generalized forces* are expressed as

$$\begin{array}{lll} 1. & p^{(i)}[\delta z_A, \delta\mathbf{u}] & = \pi\delta z_A - \boldsymbol{\xi}\cdot\nabla\delta z_A - \boldsymbol{\sigma} : \nabla\delta\mathbf{u} \\ 2. & p^{(e)}[\delta z_A, \delta\mathbf{u}] & = \gamma\delta z_A + \boldsymbol{\gamma}\cdot\nabla\delta z_A + \mathbf{f}\cdot\delta\mathbf{u}. \end{array} \tag{4}$$

Here $\boldsymbol{\sigma}$ is the Cauchy stress tensor, and $\mathbf{f}$ the volumetric density of force. The external microforces are represented by the scalar γ and the vector $\boldsymbol{\gamma}$ as introduced in GURTIN [5]. Furthermore, the *virtual power density of generalized contact forces* reads

$$p^{(c)}[\delta z_A, \delta\mathbf{u}] = \zeta\delta z_A + \mathbf{t}\cdot\delta\mathbf{u}, \tag{5}$$

where ζ is the *surface density of microtraction* (a scalar) and $\mathbf{t}$ the *surface density of cohesion forces* (a tensor). ζ and $\mathbf{t}$ are two generalized contact forces applied to the body for the purely mechanical part over the boundary.

Analogously to the power relations (3)-(5) for the macroscopic case the power relations for the mesoscopic case can be formulated with the virtual order parameter $\delta\phi$ instead of δz_A, for brevity not shown here.

Assuming that no inertial microforces exist, under the condition of the principle of virtual power, the virtual powers of externally and internally acting forces must be balanced on any subdomain $\mathcal{D} \subset V$, for any choice of the virtual phase fraction and displacement fields:

$$\mathcal{P}^{(i)}[\delta z_A, \delta\mathbf{u}, \mathcal{D}] + \mathcal{P}^{(c)}[\delta z_A, \delta\mathbf{u}, \mathcal{D}] + \mathcal{P}^{(e)}[\delta z_A, \delta\mathbf{u}, \mathcal{D}] = 0, \quad \forall \delta z_A, \forall \delta\mathbf{u}, \forall \mathcal{D} \subset V. \tag{6}$$

Inserting relations (3)-(5) into Eq.(6) one obtains

$$\begin{aligned} &\int_{\mathcal{D}} (\pi + \nabla \cdot \boldsymbol{\xi} + \gamma - \nabla \cdot \boldsymbol{\gamma}) \delta z_A + (\nabla \cdot \boldsymbol{\sigma}) + \mathbf{f}) \cdot \delta\mathbf{u} \; dv \\ &\qquad + \int_{\partial\mathcal{D}} (\zeta - \boldsymbol{\xi} \cdot \mathbf{n}) \delta z_A + (\mathbf{t} - \boldsymbol{\sigma} \cdot \mathbf{n}) \cdot \delta\mathbf{u} \; ds = 0. \end{aligned} \tag{7}$$

Thus, we obtain firstly the balance equation associated with phase volume fraction z_A (Eq.8.1) and boundary condition (Eq.8.2) for the generalized microtration vector, and secondly the classical local static equilibrium (Eq.8.3) and the associated boundary condition (Eq.8.4):

$$\begin{aligned} &1. \;\; \nabla \cdot (\boldsymbol{\xi} - \boldsymbol{\gamma}) + \pi + \gamma = 0 \quad \text{in} \;\; V, \qquad &&2. \;\; \zeta = (\boldsymbol{\xi} - \boldsymbol{\gamma}) \cdot \mathbf{n} \;\; \text{on} \;\; \partial V, \\ &3. \;\; \nabla \cdot \boldsymbol{\sigma} + \mathbf{f} = 0 \;\; \text{in} \;\; V, &&4. \;\; \mathbf{t} = \boldsymbol{\sigma} \cdot \mathbf{n} \;\; \text{on} \;\; \partial V. \end{aligned} \tag{8}$$

For the sake of brevity we assume $\gamma = 0$ and $\boldsymbol{\gamma} = \mathbf{0}$. Therefore, from Eq.(8.1) we obtain the relation

$$\nabla \cdot \boldsymbol{\xi} + \pi = 0 \;\; \text{in} \quad V. \tag{9}$$

The local balance of energy and the entropy principle are given by, see e.g. Forest *et al.* [4]

$$\begin{aligned} &1. \qquad \rho\,\dot{\epsilon} + \operatorname{div}\mathbf{q} \;\; = p^{(i)} + \rho\, r_\theta \qquad \text{in} \;\; V, \\ &2. \qquad -\rho\,\dot{\Psi} + \rho\,\theta\,\dot{\eta} + p^{(i)} - \frac{1}{\theta}\,\mathbf{q} \cdot \nabla\theta \;\; \geq 0. \qquad \text{in} \;\; V. \end{aligned} \tag{10}$$

In addition to the above notations we use: ρ - density, ϵ-specific internal energy, $\mathbf{q}$ - heat-flux density vector, r_θ - mass density of heat supply. Analogously to Eq. (4.1) we have

$$p^{(i)}[\dot{z}_A, \dot{\mathbf{u}}] = -\pi \dot{z}_A + \boldsymbol{\xi} \cdot \nabla \dot{z}_A + \boldsymbol{\sigma} : \dot{\boldsymbol{\varepsilon}}. \tag{11}$$

We also recall, that inequality (10.2) is known as the *Clausius-Duhem inequality*.

Finally we remark that relations (6)-(11) hold also for the mesoscopic case by replacing the phase volume fraction z_A and its virtual counterpart δz_A by the order parameter ϕ and its virtual counterpart $\delta\phi$.

2.2 Constitutive Framework

2.2.1 Multi-mechanism model at the macrolevel

We assume the following functional relation for the Helmholtz free energy Ψ

$$\Psi = \Psi[\boldsymbol{\varepsilon}^{el}, \underline{q}, z_A, \nabla z_A, \theta], \tag{12}$$

where $\boldsymbol{\varepsilon}^{el}$ is the elastic strain tensor, $\underline{q} = [q_i, \ldots, q_{n_q}]$ is a vector of hardening internal variables of strain type. Next, we introduce constitutive relations for the Cauchy stress tensor $\boldsymbol{\sigma}$ and the entropy η and define thermodynamic forces $\underline{Q} = [Q_1, Q_2, \ldots, Q_{n_q}]^T$

$$\begin{aligned} &1. \quad \boldsymbol{\sigma} = \rho \frac{\partial \Psi}{\partial \boldsymbol{\varepsilon}^{el}}, \quad 2. \quad \eta = -\frac{\partial \Psi}{\partial \theta}, \quad 3. \quad \underline{Q} = \rho \frac{\partial \Psi}{\partial \underline{q}}, \\ &4. \quad Z_A = \rho \frac{\partial \Psi}{\partial z_A} + \pi. \quad 5. \quad \boldsymbol{\xi} = \rho \frac{\partial \Psi}{\partial \nabla z_A}. \end{aligned} \tag{13}$$

The thermodynamic forces Q_i are called hardening stresses and the quantity Z_A is named chemical force. The relations (13.1-2) result from the Clausius-Duhem inequality by standard arguments, see e.g. [9]. The following inequalities are sufficient for validity of the Clausius-Duhem inequality (10.2):

$$1. \;\; \mathcal{D}^i = \boldsymbol{\sigma} : \dot{\boldsymbol{\varepsilon}}^{in} - \underline{Q}\ \underline{\dot{q}} - Z_A \dot{z}_A \geq 0, \qquad 2. \;\; \mathcal{D}^\theta = -\frac{1}{\theta} \mathbf{q} \cdot \nabla \theta \geq 0. \tag{14}$$

A common approach for the heat flux vector in Eq.(14.2) is the Fourier-law $\mathbf{q} = -\lambda_\theta \nabla \theta$, where λ_θ is a non-negative heat conduction coefficient. In a general setting it is necessary to formulate evolution equations

$$\begin{aligned} &1. \quad \dot{\boldsymbol{\varepsilon}}^{in} = \dot{\boldsymbol{\varepsilon}}^{in}\ [\boldsymbol{\sigma}, \underline{Q}, Z_A, \underline{q}, z_A, \nabla z_A, \theta], \quad 2. \quad \underline{\dot{q}} = \underline{\dot{q}}\ [\boldsymbol{\sigma}, \underline{Q}, Z_A, \underline{q}, z_A, \nabla z_A, \theta], \\ &3. \quad \dot{z}_A = \dot{z}_A\ [\boldsymbol{\sigma}, \underline{Q}, Z_A, \underline{q}, z_A, \nabla z_A, \theta], \end{aligned} \tag{15}$$

which are in accordance with the Clausius-Planck inequality (14.1), such that the model under consideration becomes thermodynamical consistent.

Based on the above gradient type macroscopic framework, in our new work [2] a multi-mechanism model is developed for simulation of visco-plastic material behavior accompanied by gradient phase transformation. To this end the classical Johnson-Cook model is extended to take into account visco-plastic asymmetric effects and transformation induced plasticity, for more details we refer to [10]. As a main idea, evolution equations for the phase fractions of austenite and martensite are formulated with the extended gradient term. For the case of austenitic transformation an approach due to Leblond and Devaux [8] and for the case of retransformation the classical Koistinen-Marburger [7] approach are used. Both approaches are extended by the gradient of austenite phase fraction ∇z_A.

2.2.2 Phase-field model at the mesolevel

The mesoscopic model is based on the phase field approach in [4]. The free energy density Ψ is given by $\Psi = \Psi[\boldsymbol{\varepsilon}^{el}, \underline{V}_k, \phi, \nabla \phi, \theta]$, where $\underline{V}_k$ is a vector of hardening

internal variables of strain type. Next, we define thermodynamic forces:

$$\begin{aligned} &1. \quad \boldsymbol{\sigma} = \rho \frac{\partial \Psi}{\partial \boldsymbol{\varepsilon}^{el}}, \quad 2. \quad \eta = -\frac{\partial \Psi}{\partial \theta}, \quad 3. \quad \underline{A}_k = \rho \frac{\partial \Psi}{\underline{V}_k}, \\ &4. \quad \pi_{dis} = \pi + \rho \frac{\partial \Psi}{\partial \phi}, \quad 5. \quad \boldsymbol{\xi} = \rho \frac{\partial \Psi}{\partial \nabla \phi}. \end{aligned} \tag{16}$$

The thermodynamic forces $\underline{A}_k = [A_{k1}, A_{k2}, \ldots, A_{kn}]^T$ are called *hardening stresses* and the quantity π_{dis} is named *chemical force*. The following inequalities are sufficient for the validity of the Clausius-Duhem inequality

$$1. \;\; \mathcal{D}^i = \boldsymbol{\sigma} : \dot{\boldsymbol{\varepsilon}}^{in} - \underline{V}_k \dot{\underline{A}}_k - \pi_{dis} \dot{\phi} \geq 0, \qquad 2. \;\; \mathcal{D}^\theta = -\frac{1}{\theta} \mathbf{q} \cdot \nabla \theta \geq 0. \tag{17}$$

As for macroscopic modelling we formulate the evolution equations $\dot{\boldsymbol{\varepsilon}}^{in} = \dot{\boldsymbol{\varepsilon}}^{in}\,[\boldsymbol{\varepsilon}^{el}, \underline{V}_k, \phi, \nabla\phi, \theta]$, $\dot{\underline{V}}_k = \dot{\underline{V}}_k\,[\boldsymbol{\varepsilon}^{el}, \underline{V}_k, \phi, \nabla\phi, \theta]$ and $\dot{\phi} = \dot{\phi}\,[\boldsymbol{\varepsilon}^{el}, \underline{V}_k, \phi, \nabla\phi, \theta]$, which are in accordance with Clausius-Planck inequality (17), such that the model under consideration becomes thermodynamical consistent.

3 Representative examples

In this section two numerical examples are presented.

3.1 Macroscopic modelling of cutting simulation

In the first example a cutting process is investigated in order to test the macroscopic model. The geometry and the finite-element discretization are shown in Figure 1. The geometry of the tool is described be a negative rake angle $\alpha = -6°$, a clearance angle $\beta = 6°$ as in the previous work [10]. The dimensions of the workpiece (2D) are the length of 2000 μm and the height of 400 μm. The boundary conditions on the workpiece are applied at the bottom, left side, the cutting face as well as the right side below the cutting surface, while the tool moves in horizontal direction with constant velocity $v = 40$ ms^{-1}. The initial conditions assume room temperature, and a conventional cooling condition is applied on the surfaces of the workpiece.

The macroscopic model is implemented as a user-defined subroutine (VUEL) on the element level and linked to Abaqus v6.11. Large strain modelling is taken into account by ABAQUS with an update Lagrange formulation. Based on the parameter identification for the material DIN 100Cr6 (without the gradient term), the macroscopic model is applied to the material behavior of the workpiece as shown in Figure 1 (see [2] for more details). To a separation layer we assign a shear failure criterion for separating the chip from the workpiece. The tool is modeled as purely elastic with high elastic modulus.

The results are presented in Figure 2. a) and b) show that high stresses and temperatures appear at the cutting edge, and high residual stresses at the chip top. c) shows different stress zones indicated by the stress mode factor, which is introduced in [10], for consideration of the asymmetric effects. Furthermore, the influence of the gradient term for phase transformation is demonstrated. d), e) and f) show the austenite phase fraction (the rectangle in d) visualises a representative volume element for the next example on mesoscopic modelling), its gradient in horizontal and

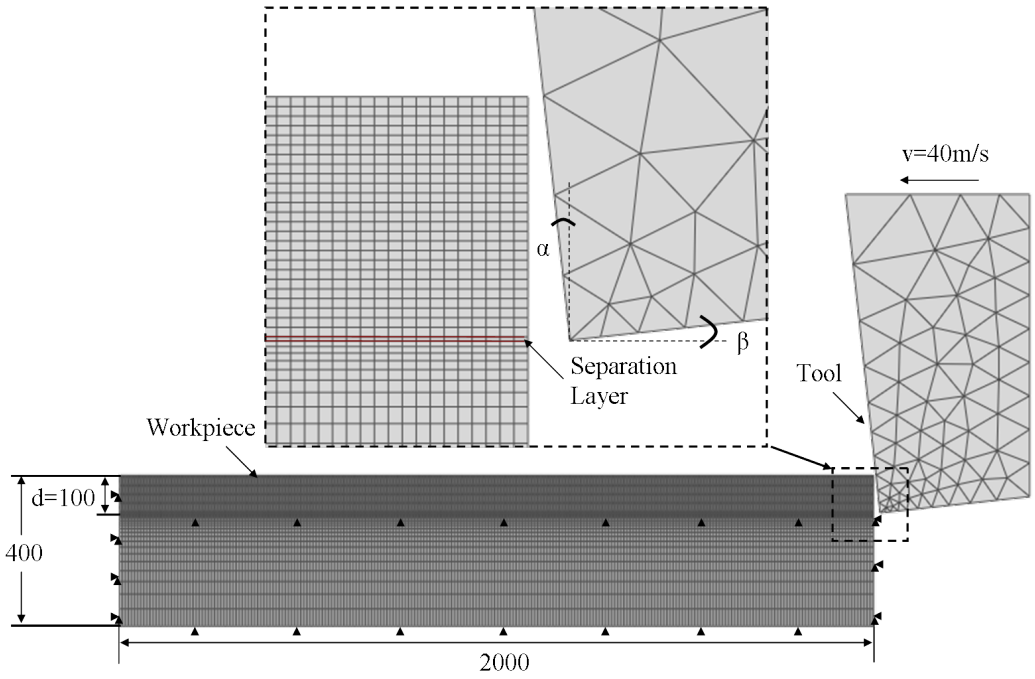

Figure 1: Cutting simulation: Geometry and finite-element discretization

vertical direction without influence of the gradient term. In comparison, g), h) and i) are under the influence of the gradient term. The austenite phase fraction and its gradients are clearly different because of the influence of the extended gradient term. In the summary in Section 4 we comment on future challenges regarding the gradient term and its identification.

3.2 Mesoscopic modelling of phase-field simulation

The second example intends to simulate the thermo-mechanic coupling in the representative volume element in Figure 2 d). The element is firstly heated from above and then cooled during a cutting process (see temperature illustration in Figure 2.a). As initial condition the phase field is assigned to be martensite with a few randomly distributed nucleuses of austenite.

Figure 3 shows the temperature (a), the martensite fraction (b), the von-Mises stress (c) and the equivalent plastic strain (d). The phase transition is controlled by the temperature. Martensite is a purely elastic phase whereas austenite is implemented with von-Mises plasticity. The results demonstrate that the von-Mises stress in martensite is much higher than in austenite and the equivalent plastic strain only grows in austenite.

4 Summary and conclusions

Macroscopic modelling: Based on the concept of generalized stresses in Forest *et al.* [4], we extended a macroscopic model developed in our previous work [10] with a gradient term. This general model has been specialized and applied to a cutting process in steel production. Furthermore, the model is applied for a cutting

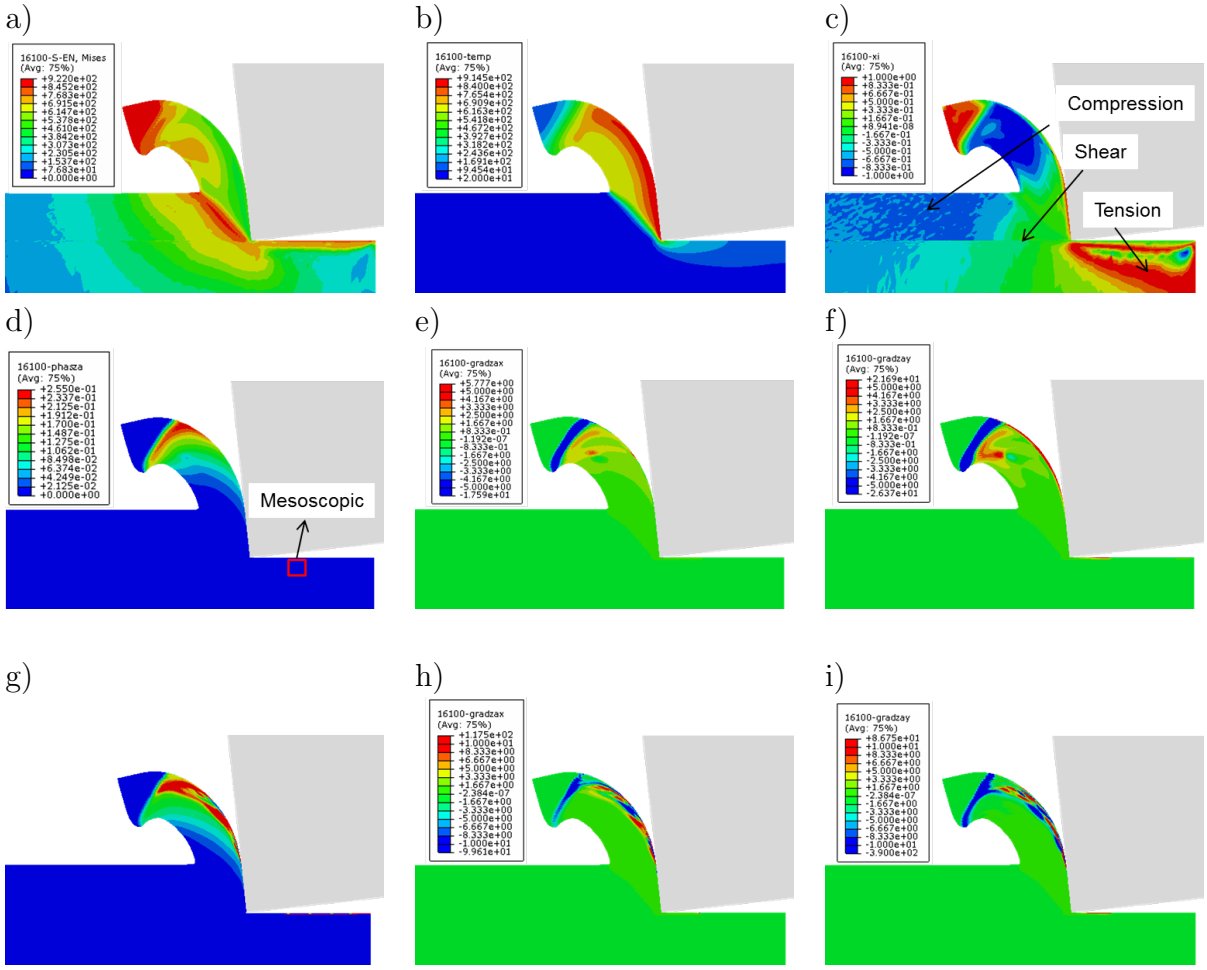

Figure 2: Cutting simulation: Contours of a) von-Mises stress, b) temperature, c) stress mode factor, d) and g) austenite volume fraction(the rectangle in d) visualise a representative volume element for the next example on mesoscopic modelling), e) and h) gradient of z_A in horizontal direction, f) and i) gradient of z_A in vertical direction, d), e) and f) show without, and g), h) and i) with influence of the gradient term

simulation, and the influence of the gradient term is studied.

Concerning future works, a big challenge is the identification of the gradient term on the basis of experiments. The studied material DIN 100Cr6 has a carbon content from 0.93 to 1.05%, which leads to a stabilisation of austenit after the cooling in a martensite-austenite-martensite transformation during a cutting process. The quantities and space distribution of the rest austenite can be measured by using Electron Backscatter Diffraction (EBSD). According to this aspect we intend to identify the gradient term. Furthermore, the macroscopic model will be extended with hardness dependency according to Umbrello *et al.* [14]. For incorporation of visco-plastic asymmetry a varied strain-rate form (Huh-Kang [6]) with better description of strain-rate dependency will be integrated in our model.

Mesoscopic modelling: Based on the same theory as the macroscopic case, the concept of generalized stresses, a phase-field model at the mesolevel is implemented and investigated for a phase-field simulation with mechanical coupling. A possible extension of the phase-field model is the consideration of carbon diffusion, which is

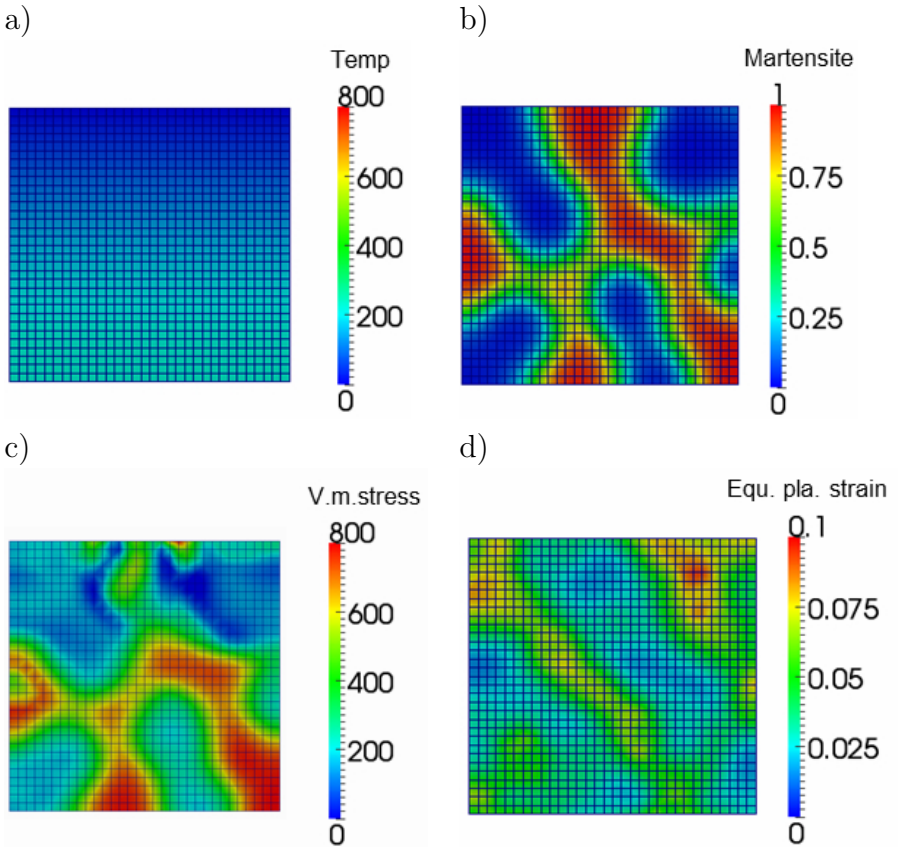

Figure 3: Phase-field modelling: a) temperature, b) martensite volume fraction, c) von-Mises stress and d) equivalent plastic strain.

of interest for the austenitic phase transformation.

Acknowledgement

This paper is based on investigations of SPP 1480, which is kindly supported by the Deutsche Forschungsgemeinschaft (DFG).

REFERENCES

[1] Ammar, K.; Appolaire, B.; Cailletaud, G.; Feyel, F.; and Forest, S., 2009, Finite element formulation of a phase field model based on the concept of generalized stresses, Computational Materials Sciences, **45** 800-805

[2] Cheng, C; Mahnken, R., 2014, A multi-mechanism model for cutting simulation based on the concept of generalized stresses, in preparation.

[3] Dudzinski, D., Molinari, A., 1997, Modelling of cutting for viscoplastic materials, *Int. J. Mech. Sci.*, **39**, 4, 369-389

[4] Forest, S.; Ammar, K.; Appolaire, B., 2011, Micromorphic vs. Phase-Field Approaches for gradient Viscoplasticity and Phase Transformations, Lecture Notes in Applied and Computational Mechanics **59** (2011), S. 69 - 88

[5] Gurtin, M., 1996, Generalized Ginzburg-Landau and Cahn-Hilliard equations based on a microforce balance, Physica D, 92:178-192

[6] Huh, H.; Kang, W.J., 2002, Crash-worthiness assessment of thin-walled structures with the high-strength steel sheet, Int. J. of Veh. Des., **30**, Numbers 1/2

[7] Koistinen, D.P.; Marburger, R.E., 1959, A general equation prescribing the extent of the austenite-martensite transformation in pure iron-carbon alloys and plain carbon steels, Acta Metallica, **7**, 59-60

[8] Leblond, J.B.; Devaux, J., 1984, A new kinetic model for anisothermal metallurgical transformations in steels including effect of austenite grain size, Acta Metallurgica, **32**, 137-146

[9] Mahnken, R.; Wolff, M.; Schneidt, A.; Böhm, M., Multi-Phase Transformations at Large Strains - Thermodynamic Framework and Simulation, International Journal of Plasticity 39 (2012) 1-26

[10] Mahnken, R.; Wolff, M.; Cheng, C., A multi-mechanism model for cutting simulations combining visco-plastic asymmetry and phase transformation, Int. J. Solids Struct. (2013), Vol. 50, S. 3045-3066

[11] Marusich, T., Ortiz, M.: 1995, Modelling and Simulation of High-Speed Machining, Int. J. Num. Meths. Eng.,Vol. 38, 3675-3694

[12] Ramesh, A; Melkote, S.N., 2007, Modeling of white layer formaion under thermally dominant conditions in orthogonal machining of hardened AISI 52100 steel, International Journal of Machine Tools and Manufacture, **48**, 402–414

[13] Sievert, R.; Noack, H.D.; Hamann, A.; Lwe, P.; Singh, K.N.; Knecke, G.; Clos, R.; Schreppel, U.; Veit, P.; Uhlmann, E.; Zettier, R., 2003, Simulation der Spansegmentierung beim Hochgeschwindigkeits- Zerspanen unter Berücksichtigung duktiler Schädigung, *Technische Mechanik*, **23**, 2-4, 216–233

[14] Umbrello, D.; Hua, J.; Shivpuri, R., 2004, Hardness-based flow stress and fracture models for numerical simulation of hard machining AISI 52100 bearing steel, Ma. Sci. Eng, **A 374**, 90-100

[15] Zerilli, F.J.; Armstrong, R.W., 1987, Dislocation-mechanics-based constitutive relations for material dynamics calculations, Journal of Applied Physics, **61**, (5): 1816